Electron detachment of Si^- by He, Ne, and Ar

H. Luna, S. D. Magalhães, J. C. Acquadro, M. H. P. Martins, W. M. S. Santos, Ginette Jalbert, L. F. S. Coelho, and N. V. de Castro Faria

Instituto de Física, Universidade Federal do Rio de Janeiro, Caixa Postal 68528, Rio de Janeiro, 21945-970, Rio de Janeiro, Brazil

(Received 1 June 2000; published 10 January 2001)

The cross sections for electron detachment of Si^- were measured for He, Ne, and Ar targets at relative velocities in the 0.25–1.4 a.u. range. Argon target cross sections were measured using Si^- ions from two different origins, the results agreeing well with each other and with literature values. The velocity dependence of the Si^- cross sections is strikingly similar to that of known H^- results, with the former being consistently larger than the latter and, at large velocities, differing by a multiplicative constant.

DOI: 10.1103/PhysRevA.63.022705 PACS number(s): 34.50.Fa, 34.90.+q

I. INTRODUCTION

The large majority of atomic species form stable negative ions in the gas phase. Detachment of electrons from these atomic (and also molecular) negative charged ions (in photon, electron, or heavier particle collisions) has been studied for almost five decades [1], as seen in some extensive reviews [2]. Electron detachment in collisions with atoms has been studied in the keV and MeV energy ranges, mostly in the last two decades [3,4], the interest being not only for basic science but also for its applications in fusion research, studies of stellar atmospheres, astrochemistry, materials science, etc. One such application, for instance, is in ion beam deposition in insulators, where the charging-up phenomenon may be either avoided or diminished [5].

In spite of these several areas of relevance, measuring these cross sections has been limited by the lack of accelerators able to impinge fast negative ions on gaseous targets. In fact, negative ions are routinely obtained from standard cesium vapor sputtering ion sources and injected into the first stage of tandem accelerators [6], but these fast negative ion beams are used only as a way to produce singly or multiply charged positive ion beams after collisional stripping by a gas or a carbon foil. Recently [7] we proposed a technique for studying the collisional detachment of fast negative ions in a tandem accelerator, using the gas stripper itself as a target, which opened possibilities in this area.

Although collisional detachment on atomic and molecular targets has been measured for several anion species, as described in the literature [8], by far the most studied case is H^- detachment in collisions with He, Ne, and Ar atoms [9,10]. One important feature is that, for velocities smaller than 0.75 a.u., He presents a larger cross section than Ne. This fact is described by Olson and Liu [11] in the framework of transitions among XH^- and XH intersecting quasimolecular states, where X represent He or Ne. They calculated these potential energy curves and observed distinct behaviors in the helium and neon cases, with the former presenting a crossing of states at small internuclear separation, while in the latter the states do not intersect, but merge at low internuclear separations. Furthermore, alkali-metal anions had their detachment cross sections in noble gases measured by Andersen *et al.* [12], who proposed a universal fitting in terms of the H^- cross section and target-independent multiplicative factors. A surprisingly good scaling was then achieved for velocities over 0.5 a.u., which was attributed to their similar ns^2 configurations.

Systematic studies of the collisional detachment of other groups of the periodic table have not yet been made. Semiconductor anions, for instance, present the np^3 configuration and, besides the intrinsic and applied relevance of their detachment measurements, they are almost the only ones to present bound excited states. The Si^- ion, for instance, has three electrons in the $3p^3$ subshell and, in addition to the ground $^4S_{3/2}$ level, presents excited long lived ^2D and ^2P terms [13–15]. As measured by Scheer *et al.* [13], the $^2D_{3/2,5/2}$ binding energies are respectively equal to 0.527 and 0.525 eV while the ^2P term has a very small binding energy, of the order of 29 meV. The population of these metastable states in a beam formed by a sputtering ion source was discussed in two experimental works [13,16]. Scheer *et al.* [13] pointed out that the excited ^2D Si^- population corresponded, approximately, to a few nA out of the μA total Si^- beam current. Balling *et al.* [16] also noted that the metastable population is very low ($<2\%$).

The state population of sputtered anions could be roughly estimated using the Boltzmann factor, the main problem being to estimate an effective temperature. Norskov and Lundqvist [18] have estimated an effective temperature of 9000 K for the typical Cu^+ sputtering case. This value, applied to the Si^- case, would give a ^2D population, relative to the ground state, of about 30%. On the other hand, considering the effective temperature as equal to the room temperature, we obtain the result that 99% of the anions are in the ground state.

As already stated, the Si^- ^2P state has a binding energy of 29 meV. The population of this weakly bound state was found to be very small due to the quenching induced by the high electric fields produced by irregularities at the sputtered target surface, which may exceed 1 MV/m [19].

The measurement of detachment cross sections of Si^- colliding with atoms and their comparison with the well known values for H^-, which has a binding energy of 0.75 eV, could give a qualitative indication of the beam composition. Evidence may also come when Si^- anions produced by different processes, like the fragmentation of Si_2^- or electron capture by Si, are employed in the detachment experiments.

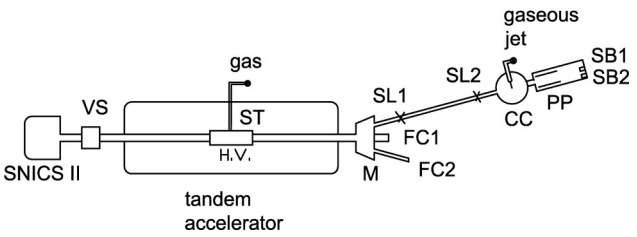

FIG. 1. Experimental setup. SNICS II: sputtering ion source; VS: velocity selector; ST: stripper gas cell; M: magnet; FC1 and FC2: Faraday cups used in method A; SL1 and SL2: collimating slits (15° beamline); CC: collision chamber (method B); PP: parallel plates; SB1 and SB2: surface barrier detectors.

Algebraic approximations to Hartree-Fock wave functions of Si^- are available in the literature [20] but, as far as the authors are aware, there are no calculated results for the collisional detachment cross sections. Considering this fact, a simplified model that describes the detachment process as the scattering of the (assumed free) projectile electron by the target [21] and is expected to be valid for energy transfers, as measured in the projectile nucleus rest frame, much larger than the ionization energy, could be used in the interpretation of the projectile dependence of the high-velocity region detachment results.

In order to test all the particularities verified for the H^- case we measured the detachment cross sections of Si^- in collisions with He, Ne, and Ar for velocities in the interval 0.25–1.4 a.u. On the experimental side, the silicon anion can be produced in standard cesium sputtering ion sources [13,17,16] but, as described in the next section, these measurements were also performed with Si^- ions produced by collisional dissociation of Si_2^+ ions, presenting a possibly different metastable component. The cross sections were extracted using both the attenuation and the growth techniques.

II. EXPERIMENTAL APPARATUS AND MEASUREMENT TECHNIQUES

We have done two different sets of experiments: (1) collision of anions produced in a sputtering ion source with a gas target (method A); and (2) collision of anions produced by a secondary process with a gas jet target (method B). Both experimental arrangements are presented in Fig. 1. The total (and absolute) detachment cross sections, in both cases, were extracted from the exponential decay curves obtained when the target pressure was varied. In the second arrangement the growth rate method was employed to measure the neutral and positive beams that correspond to the loss of one or two electrons. Our accelerator's beam current may be considered constant for time intervals of some minutes, simplifying the normalization of the incident beam by avoiding the use of a rotating beam chopper, as was done in Ref. [3]. In all cases, we measured the total beam just before and after each measurement and the average was taken as the incident beam, with variations being observed in the 1–4 % range.

In the first set of experiments (method A) we employed the method developed in Refs. [7]. The Si^- beam is produced in the cesium sputtering ion source (SNICS II) [17],

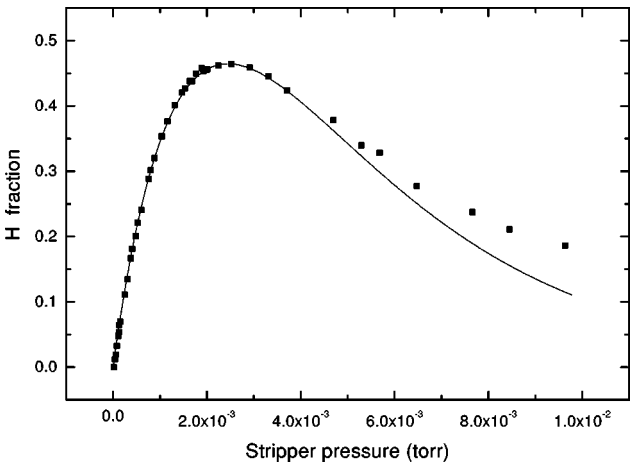

FIG. 2. Measured H beam fraction (black squares) and the corresponding theoretical calculations using known detachment cross sections of 1 Mev H^- colliding with Ar (solid line).

preaccelerated to a kinetic energy E_p, and then mass selected by a Wien filter. Our typical cathode and preaccelerating voltages were, respectively, 5 kV and 15 kV. The beam enters the first stage of the tandem accelerator 5SDH (NEC) of the IF-UFRJ and reaches the central terminal with energy E_p+eV, where V is the terminal potential (1.7 MV maximum), ranging in our experiment from 20 kV to 1.3 MV. The beam particles can then collide with the atoms (or molecules) of the gas target (''stripper''). The gas is introduced from outside through a pressurized insulating tube, the target pressure being regulated by an externally controllable mechanical valve. In the second stage of the accelerator, the beam particles will be decelerated (the Si^- case), or continue with the velocity obtained in the first stage (the Si case), or, finally, be accelerated (the Si^{n+} case). In the case of Si^-, this ion leaves the accelerator with the same velocity as it gets from preacceleration, and its subsequent magnetic selection is under a less stringent rigidity limitation. After the magnet the Si^- beam current is measured on a Faraday cup.

A direct reading of the stripper pressure is not possible, and its value is obtained by applying a measured functional relation with the grounded end pressure, as described in Refs. [7]. Briefly, that functional relation is obtained, first, by employing known charge-changing cross sections for hydrogen ions colliding with He, Ne, and Ar to obtain the neutral beam fraction after traversing the stripper gas target as a function of the gas pressure [22], and then by comparing this analytical curve to the neutral fraction, measured in a Faraday cup, as a function of the pressure at the exit of the tandem accelerator.

The quality of the normalization pressure technique is shown in Fig. 2, where the neutral fraction is displayed as a function of the true target pressure. The solid line was calculated using known experimental cross sections [3] and the points are our measured values, multiplied by one vertical and one horizonal adjustable factors to give the best fit to the theoretical values from the low measured pressures to the maximum of the neutral fraction. The uncertainties come mainly from the known cross sections used in the theoretical calculations, and the systematic deviation for high pressures

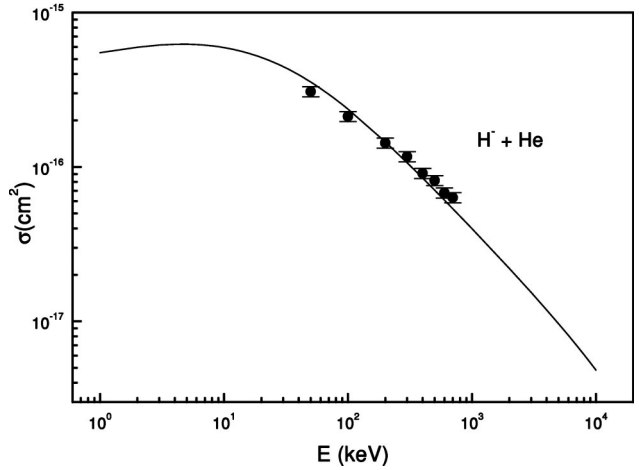

FIG. 3. Our measured cross sections (black circles) for H^- incident on He compared to averaged values taken from Ref. [9].

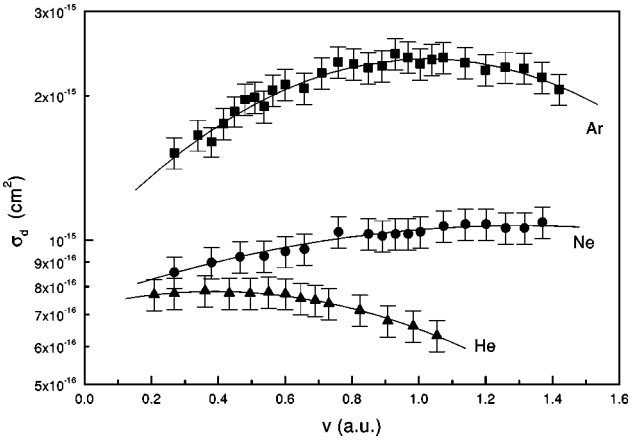

FIG. 4. Total electron detachment cross section for Si^- incident on He (triangles), Ne (circles), and Ar (squares) measured by method A as a function of the relative velocity in atomic units. The solid lines were drawn only to guide the eyes.

is due to the charge changing in the bad vacuum of the tube at the accelerator second stage, and for this reason they were not employed in our fit. In fact there are two additional contributions to the neutral component, both coming from the second stage of the tandem, where H^- may undergo single electron loss collisions on the residual gas and H^+ may undergo capture, and these collision processes are more relevant at large stripper pressures. When we adjust both theoretical curve and experimental data, we have a linear correspondence between the stripper pressure and the read grounded end pressure, for stripper pressure lower than 3×10^{-3} Torr. The deviation occurs at pressures higher than 5×10^{-3} Torr. Therefore, this linear relation is used to achieve the stripper density as discussed in Refs. [7].

The good quality of results is better seen in the values we get for the total detachment cross sections of H^- in collision with He, presented in Fig. 3 together with a semiempirical fit of the known experimental results presented in Ref. [9].

In the second series of experiments (method B) we employed a different method to produce the Si^- ions. Briefly, Si_2^+ ions are formed in the stripper at the high-voltage terminal and accelerated in the second stage of the tandem accelerator. Si^- ions are then produced by collisional dissociation of Si_2^+ ions on the residual gas in a chamber. This chamber is placed immediately before the magnet switch (M) and these ions are subsequently mass selected. In order to achieve a Si^- beam of a few hundred particles per second we needed a nanoampere Si_2^+ beam. After collimation by two set of slits, SL1 and SL2, with 0.4 mm apertures and placed 2 m apart, the Si^- beam crosses a gas jet target placed in the collision chamber (CC). The pressure of the target was also normalized to the known $H^-\rightarrow H$ single electron detachment results. The particles were detected by two surface barrier detectors, SB1 (neutrals) and SB2 (charged particles), after separation by an electric field applied between two parallel plates (PP), each charge state being measured on a different run.

III. RESULTS AND DISCUSSION

The results obtained using method A for the total detachment cross sections σ_d^A are shown in Fig. 4, for He, Ne, and Ar targets. The solid lines (second degree polynomials) were drawn only to guide the eyes. The smaller maximum velocity in the He case is due to the lower maximum voltage used, in order to avoid an electrical discharge in the gas feedthrough tube.

The results obtained using method B for the total, single and double detachment cross sections σ_d^B, σ_{10}^-, and σ_{11}^-, respectively, are shown on Table I for an Ar target. The range of projectile velocities, 0.65 to 1.07 a.u., was limited by the surface barrier detector noise and by the magnetic selector. In all results an average uncertainty of $\pm7-8\,\%$ must be assigned to the absolute values of the measured cross sections, coming mainly from the fitting procedure and

TABLE I. Comparison of the total detachment cross sections (in 10^{-15} cm^2) of Si^- colliding with Ar obtained with two different methods, σ_d^A and σ_d^B. Single and double electron detachment cross sections were obtained with the method B.

v(a.u.)	0.65	0.75	0.83	0.93	1.00	1.07
σ_d^A	2.07±0.16	2.35±0.18	2.29±0.17	2.45±0.19	2.33±0.18	2.40±0.19
σ_d^B			2.03±0.15	2.50±0.19	2.15±0.16	2.17±0.16
σ_{10}^-	1.08±0.08	1.11±0.08	1.14±0.08	1.31±0.10	1.16±0.09	1.01±0.08
σ_{11}^-			0.43±0.03	0.61±0.05	0.45±0.03	0.69±0.05

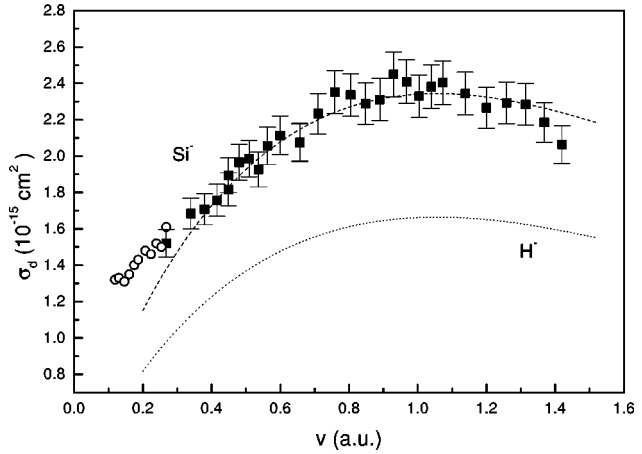

FIG. 5. Total electron detachment cross sections for Si^- incident on Ar measured by method A (black squares) and for H^- incident on Ar (dotted line) [9]. Dashed line is the best fit of Si^- data by the expression $\sigma_d^{Si^-}(v)=c\sigma_d^{H^-}(v)$. The low-velocity data (open circles) were taken from Ref. [5].

from the pressure measurement.

The measurement of the total detachment cross sections in Ar, with beams of different origins and analyzed by distinct techniques, led to σ_d^A and σ_d^B values that present no significant differences. This can be seen in Table I where, for the sake of comparison, the total cross sections obtained by the first method are also shown. This agreement suggests that the composition of the Si^- beam is not so different for the two cases. Our results (method A) also agree very well with values found in the literature for argon at velocities lower than 0.27 a.u. [5], as shown in Fig. 5.

Table I also shows that the single and double electron loss cross sections are about one half and one fourth of the total electron loss cross section. The triple electron loss was also measured using method B at the higher end of the velocity range, $v=1.07$ a.u., obtaining $\sigma_{12}^{-}=(0.30\pm0.02)\times10^{-15}$ cm^2. We observe that the sum of the three channels (σ_{10}^{-}, σ_{11}^{-}, and σ_{12}^{-}) is equal to $(2.00\pm0.15)\times10^{-15}$ cm^2, slightly underestimating the values obtained by direct measurement, $\sigma_d^A=(2.40\pm0.19)\times10^{-15}$ cm^2 and $\sigma_d^B=(2.17\pm0.16)\times10^{-15}$ cm^2. This difference, although within the error bars, may also be due to core electron loss processes, when four or more electrons are ejected. As Si^- has three equivalent $3p$ electrons [13], we can estimate that the major contribution came from these three external electrons.

Concerning now the Si^- total detachment data, our first objective was to understand rather empirically the unexpected ressemblance between the Si^- and H^- results as shown in Fig. 5 for the Ar case, and which occurs also for He and Ne. This similarity for two rather different anionic projectiles is even more impressive as, for either of the two projectiles, there is a marked target dependence.

The H^- detachment cross sections presented, in the 0.1–1.5 a.u. velocity range, have maxima around 0.44 for helium, 1.3 for neon, and 1.06 a.u. for argon. In addition, for velocities lower than 0.75 a.u., the detachment cross sections for collisions with helium become larger than for neon. A prediction of the position of the H^- cross section maxima is given by the adiabatic criterion [23], but at velocities one order of magnitude lower than the measured values, this discrepancy being partly due to the choice of a target- and projectile-independent ''adiabatic parameter'' and to the use of the binding energy as the relevant energy difference. The relevance of the binding energy as a parameter for collisional detachment processes is illustrated by the Peart *et al.* [24] and Andersen *et al.* [12] measurements. Peart *et al.* measured the electron-impact electron detachment cross section of H^-, C^-, O^-, F^-, and Na^-, obtaining maximum positions monotonically dependent on the anion binding energy. When scaled using a classical scaling law [25] all have their maxima almost at the same scaled electron velocity. On the other hand, Andersen *et al.* [12] measured the Li^-, Na^-, and K^- cross sections on noble gas targets. They were able to scale their results to the H^- cross sections by the use of simple multiplicative parameters, respectively equal to 1.4, 1.8, and 2.6, independent of the target gas, with a surprisingly good scaling which was mostly attributed to the similar ns^2 configuration of these four anions.

TABLE II. The linear fit (a,b) and purely multiplicative (c) parameters employed to match our experimental Si^- curve and the analytical fit of the H^- data [9].

Atom	$a(10^{-16}$ $cm^2)$	b	c
He	2.3	0.9	1.3
Ne	5.3	0.9	1.9
Ar	0.6	1.4	1.4

Although silicon and hydrogen possess distinct configurations and the binding energies of the ground and metastable states of Si^- are not similar to those of H^-, we believe it to be instructive to make a similar comparison. The unexpected similarity of both data curves, as shown in Fig. 5 for the Ar case, suggests the validity of a linear scaling such as

$$\sigma_d^{Si^-}(v)=a+b\sigma_d^{H^-}(v)$$

or the simpler expression

$$\sigma_d^{Si^-}(v)=c\sigma_d^{H^-}(v).$$

Table II presents the adjusted values of the constants a, b, and c for He, Ne, and Ar targets. Although the first model fits the data reasonably well in the low-velocity region, the simple multiplicative hypothesis describes the high-velocity end very well, as shown in Fig. 5 for Ar. When we try to analyze the more plausible second model, we observe that the c values are of the same order of magnitude, their averages differing by less than 24%. The fact that the parameter b is almost equal to unity in the He and Ne cases could only indicate that the low-velocity side had a large influence on the fit. A rough scaling with the inverse square of the binding energy fits the H^- case well to alkali-metal anions [12] in collision with noble gases. Although this does not occur in our case, Si^- presenting a p^3 configuration, the same simple multiplicative scaling was found to be valid.

One attempt to handle theoretically the problem of single electron loss from H and H^- interacting with a noble gas target, presented in Ref. [10], is based on a free collision type model and led to simple analytical expressions. The resulting formula shows a good agreement with experimental data in the H case, for helium and neon targets, but fails for argon and xenon at projectile velocities around the equivalent to the bound electron velocity ($v \approx v_e$). In the H^- case the description is even worse, for $v \approx v_e$, and no agreement is obtained for any target. The predicted position of the cross section maximum would occur for velocities v_{max} much larger than the least-bound-electron orbital velocity, having a monotonic power-law dependence on *Z*. Experimentally, however, as shown in Fig. 4 for Si^- and in Ref. [10] for H^-, we have $v_{max}(\mathrm{Ne}) > v_{max}(\mathrm{Ar}) > v_{max}(\mathrm{He})$ for both.

These facts prevent the use of this simplified model to interpret our data quantitatively. Instead, we could argue that this ''inversion'' reflects the behavior of the cross sections at low velocities. The maxima represent a transition from a low- to a high-velocity regime, where different mechanisms operate. In the high-velocity regime the cross section decreases with the velocity and theoretically is well described by the free collision model [10]. In contrast, in the low-velocity regime, the cross section increases.

As stated before, in the collisional detachment of H^- incident on Ne, due to the fact that the NeH^- and NeH potentials do not cross in the low-energy limit [11], the electron detachment at low velocities is inhibited, thus shifting the transitional maximum to a higher velocity and making the He and Ne cross section curves cross. Our data for the collisional detachment of Si^- incident on Ne and He seem to present the same kind of behavior, although not so pronounced. In fact, we can see in Fig. 4 that the He and Ne data are going to cross for low velocities and the maximum for Ne is shifted, just as in the H^- case, suggesting that the same mechanisms are at work.

Finally, comparing the single and double electron detachment measured by method B to the total electron detachment cross section in the case of Si^- and H^- colliding with argon, we could estimate the contribution of three or more electron detachment and the contribution of the metastable component in the case of the Si^- projectile for velocities around the maximum. It is important to remember that for H^- the single and double electron detachment account for 100% of the total electron detachment cross section, but 78% in the Si^- case. If we consider only these two contributions, we obtain values comparable to the total electron detachment cross section of H^-. Therefore the large silicon cross section could be in large part associated with the existence of three or more electrons to be detached, which are not present in the H^- case, but the presence of a metastable state in the beam is not necessarily negligible. Comparison with anions having the same configuration as Si^- is desirable to clarify the existence of metastable states in the beam.

IV. CONCLUSIONS

We have obtained total electron detachment cross sections for Si^- in collisions with He, Ne, and Ar that are correspondingly higher than the ones for H^- reported in the literature. In method A we covered a large range of velocities 0.25–1.4 a.u. We also verified that the Ar target results were not sensitive to how the anion was formed (methods A and B).

Qualitatively, the large silicon cross section was essentially explained by the detachment of three or more electrons, but the existence of a metastable contribution may not be ruled out. In order to verify this possibility and to better understand the present silicon results, a systematic study of C^- and Ge^- detachment should be done. The comparison between silicon, carbon, and germanium anions, all presenting three *p* external electrons, would then help us to interpret the metastable contribution, since all these anions present bound metastable states [13].

ACKNOWLEDGMENTS

This work was partially supported by the Brazilian agencies CNPq, FUJB, and FAPERJ.

[1] J.B. Hasted, Proc. R. Soc. London, Ser. A **212**, 235 (1952); R.C. Bilodeau, M. Scheer, and H.K. Haugen, J. Phys. B **31**, 3885 (1998); W.W. Williams, D.L. Carpenter, A.M. Covington, M.C. Koepnick, D. Calabrese, and J.S. Thompson, *ibid.* **31**, 1341 (1998); F. Robicheaux, Phys. Rev. Lett. **82**, 707 (1999); J.M. Rost, *ibid.* **82**, 1652 (1999).

[2] V.A. Esaulov, Ann. Phys. (Paris) **11**, 493 (1986); Earl W. Mc.Daniel, J.B.A. Mitchell, and M. Eugene Rudd, *Atomic Collisions: Heavy Particle Collisions* (Wiley, New York, 1994), p. 425.

[3] D.P. Almeida, N.V. de Castro Faria, F.L. Freire, Jr., E.C. Montenegro, and A.G. de Pinho, Phys. Rev. A **36**, 16 (1987).

[4] F. Melchert, M. Benner, S. Kruedener, and E. Salzborn, Nucl. Instrum. Methods Phys. Res. B **99**, 98 (1995); C.P. Safran, V.R. Bharduaj, D. Mathur, and A.K. Gupta, Chem. Phys. Lett. **259**, 415 (1996).

[5] J. Ishikawa, Rev. Sci. Instrum. **63**, 2368 (1992).

[6] W.T. Diamond, Y. Imahori, J.W. Mckay, J.S.C. Wills, and H. Schmeing, Rev. Sci. Instrum. **67**, 1404 (1996).

[7] J.C. Acquadro, Neide Gonçalves, H. Luna, R. Donangelo, N.V. de Castro Faria, O.D. Gonçalves, Ginette Jalbert, and L.F.S. Coelho, Nucl. Instrum. Methods Phys. Res. A **398**, 162 (1997); J.C. Acquadro, H. Luna, S.D. Magalhães, F. Zappa, Ginette Jalbert, E. Bessa Filho, L.F.S. Coelho, and N.V. de Castro Faria, Nucl. Instrum. Methods Phys. Res. B **171**, 373 (2000).

[8] F. Rahman and B. Hird, At. Data Nucl. Data Tables **35**, 123 (1986).

[9] Y. Nakai, T. Shirai, T. Tabata, and R. Ito, At. Data Nucl. Data Tables **37**, 69 (1987).

[10] M. Meron and B.M. Johnson, Phys. Rev. A **41**, 1365 (1990).

[11] R.E. Olson and B. Liu, Phys. Rev. A **22**, 1389 (1980).

[12] N. Andersen, T. Andersen, L. Jepsen, and J. Macek, J. Phys. B **17**, 2281 (1984).
[13] M. Scheer, R.C. Bilodeau, C.A. Brodie, and H.K. Haugen, Phys. Rev. A **58**, 2844 (1998).
[14] H. Hotop and W.C. Lineberger, J. Phys. Chem. Ref. Data **14**, 731 (1985); T. Andersen, H.K. Haugen, and H. Hotop, *ibid.* **28**, 1511 (1999).
[15] J. Thogersen, L.D. Steele, M. Scheer, C.A. Brodie, and H.K. Haugen, J. Phys. B **29**, 1323 (1996).
[16] P. Balling, P. Kristensen, H. Stapelfeldt, T. Andersen, and H.K. Haugen, J. Phys. B **26**, 3531 (1993).
[17] R. Middleton, Nucl. Instrum. Methods **144**, 373 (1977).
[18] J.K. Norskov and B.I. Lundqvist, Phys. Rev. B **19**, 5661 (1979).
[19] M-J. Nadeau and A.E. Litherland, Nucl. Instrum. Methods Phys. Res. B **52**, 387 (1990).
[20] E. Clementi and C. Roeti, At. Data Nucl. Data Tables **14**, 177 (1974); C.F. Bunge, J.A. Barrientos, and A.V. Bunge, *ibid.* **53**, 114 (1993); T. Koga, Y. Seki, A.J. Thakkar, and Tatewaki, J. Phys. B **26**, 2529 (1993); T. Koga, S. Watanabe, K. Kanayama, and R. Yasuda, J. Chem. Phys. **103**, 3000 (1995).
[21] D.P. Dewangan and H.R.J. Walters, J. Phys. B **11**, 3983 (1978).
[22] S.K. Allison, Rev. Mod. Phys. **30**, 1137 (1958).
[23] H.S.W. Massey, Rep. Prog. Phys. **12**, 248 (1949).
[24] B. Peart, R. Forrest, and K.T. Dolder, J. Phys. B **12**, L115 (1979); **12**, 847 (1979); **12**, 4155 (1979).
[25] M. Inokuti, C. Kwok-Tsang, and J.L. Dehmer, in *Abstracts of the Eleventh International Conference on the Physics of Electronic and Atomic Collisions*, edited by K. Takayanagi and N. Oda (The Society for Atomic Collisions Research, Kyoto, 1979).